LANGMUIR Article
Cite This: Langmuir 2019, 35, 12782−12791
pubs.acs.org/Langmuir

Wormlike Micelles of a Cationic Surfactant in Polar Organic Solvents: Extending Surfactant Self-Assembly to New Systems and Subzero Temperatures

Niti R. Agrawal,[†] Xiu Yue,[†,‡] Yujun Feng,[*,§] and Srinivasa R. Raghavan[*,†]

[†]Department of Chemical & Biomolecular Engineering, University of Maryland, College Park, Maryland 20742, United States
[‡]Xinjiang Technical Institute of Physics & Chemistry, Chinese Academy of Sciences, Urumqi 830011, China
[§]Polymer Research Institute, State Key Lab of Polymer Materials Engineering, Sichuan University, Chengdu 610065, China

Supporting Information

ABSTRACT: Wormlike micelles (WLMs) are long, flexible cylindrical chains formed by the self-assembly of surfactants in semidilute solutions. Scientists have been fascinated by WLMs because of their similarities to polymers, while at the same time, the viscoelastic properties of WLM solutions have made them useful in a variety of industrial applications. To date, most studies on WLMs have been performed in water (i.e., a highly polar liquid), while there are a few examples of "reverse" WLMs in oils (i.e., highly nonpolar liquids). However, in organic solvents with lower polarity than water such as glycerol, formamide, and ethylene glycol, there have been no reports of WLMs thus far. Here, we show that it is indeed possible to induce a long-tailed cationic surfactant to assemble into WLMs in several of these solvents. To form WLMs, the surfactant is combined with a "binding" salt, i.e., one with a large organic counterion that is capable of binding to the micelles. Examples of such salts include sodium salicylate and sodium tosylate, and we find self-assembly to be maximized when the surfactant and salt concentrations are near-equimolar. Interestingly, the addition of a simple, inorganic salt such as sodium chloride (NaCl) to the same surfactant does not induce WLMs in polar solvents (although it does so in water). Thus, the design rules for WLM formation in polar solvents are distinct from those in water. Aqueous WLMs have been characterized at temperatures from 25 °C and above, but few studies have examined WLMs at much lower (e.g., subzero) temperatures. Here, we have selected a surfactant with a very low Krafft point (i.e., the surfactant does not crystallize out of solution upon cooling due to a cis-unsaturation in its tail) and a low-freezing solvent, viz. a 90/10 mixture of glycerol and ethylene glycol. In these mixtures, we find evidence for WLMs that persist down to temperatures as low as −20 °C. Rheological techniques as well as small-angle neutron scattering (SANS) have been used to characterize the WLMs under these conditions. Much like their aqueous counterparts, WLMs in polar solvents show viscoelastic properties, and accordingly, these fluids could find applications as synthetic lubricants or as improved antifreezing fluids.

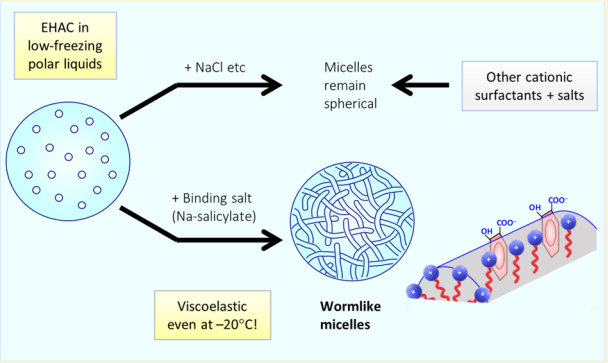

INTRODUCTION

Surfactants, that is, amphiphilic molecules with a polar headgroup and a nonpolar tail, can self-assemble into various nanoscale structures, the most common of which are micelles (Figure 1A).[1−3] A particularly interesting class of micelles is the wormlike micelles (WLMs), also called threadlike micelles.[4−8] WLMs are long, flexible cylindrical chains, with diameters around 5 nm and contour (end-to-end) lengths L ranging from 100 to 5000 nm. They are formed at relatively low surfactant concentrations (2−5 wt % or 20−100 mM). Much like chains of polymers, WLM chains become entangled in solution (Figure 1A), thereby imparting high viscosity and viscoelasticity to the solution. This ability to modulate the rheological properties has led to numerous applications for WLMs, including in oil recovery, home-care and personal care products, and as drag-reducing agents.[4,9,10] Most studies on WLMs have been conducted in water, and aqueous WLMs have been formed using cationic,[6−8,11−15] anionic,[16] and zwitterionic[17−19] surfactants. Reverse WLMs, with their tails facing out towards the solvent, have also been reported in nonpolar liquids (oils).[20−22] Lastly, some studies have been conducted on WLMs in mixtures of water and polar organic solvents (such as alcohols or diols).[23−27] To our knowledge, however, there have been no reports of WLMs in pure solvents of intermediate polarity.

Received: July 8, 2019
Revised: August 29, 2019
Published: September 17, 2019

DOI: 10.1021/acs.langmuir.9b02125
Langmuir 2019, 35, 12782−12791

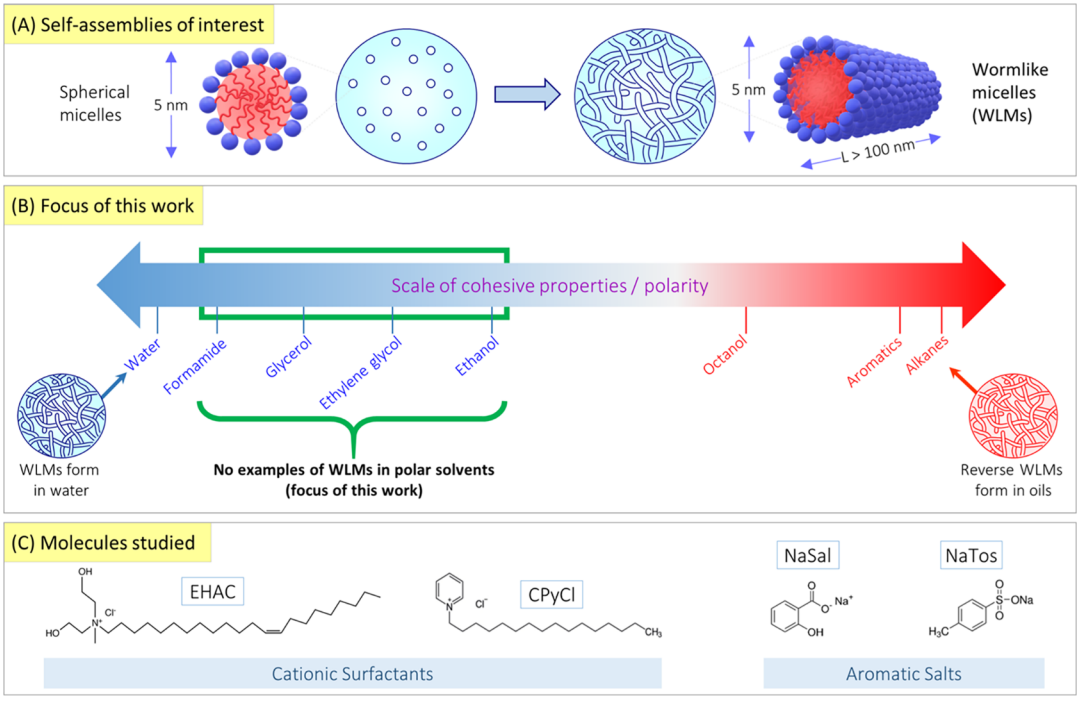

Figure 1. Overview of this study. (A) Surfactants (with their hydrophilic heads in blue and hydrophobic tails in red) can self-assemble into micelles, which can be discrete spheres (5 nm in diameter) or wormlike chains (diameter of 5 nm and length L > 100 nm). The latter, termed WLMs, are the main structures of interest here. Their formation results in the solution becoming viscoelastic. (B) Scale of solvent properties such as the cohesive energy density or polarity. WLMs have been formed in solvents at both extremes of this scale: that is, in water (highly polar) and in oils (highly nonpolar). However, in solvents with lower polarity than water, there are no reports of WLMs thus far, and that is the focus of this work. (C) Structures of molecules used in this study. These include the cationic surfactants erucyl bis(hydroxyethyl) methyl ammonium chloride (EHAC) and cetyl pyridinium chloride (CPyCl), and the aromatic salts NaSal and sodium tosylate (NaTos).

With regard to solvent polarity, it can be quantified using parameters such as the dielectric constant or the Gordon parameter, as illustrated in Figure 1B. On one extreme of such a scale is water (highly polar), whereas on the other extreme are oils such as *n*-alkanes (highly nonpolar). As the figure shows, in pure organic solvents with lower polarity than water, such as glycerol (Gly), formamide, and ethylene glycol (EG), there have been no reports of WLMs thus far. Self-assembly has been shown to occur in some of these polar solvents,[28−35] but it only results in small micelles with an aggregation number N_{agg} (i.e., the number of molecules associated into a micelle) less than about 100. The driving force for self-assembly in polar solvents is the "solvophobic effect," analogous to the hydrophobic effect,[36−39] and it too involves the nonpolar portions of surfactants segregating into the core of the micelles, whereas the polar portions remain in contact with the solvent. But the solvophobic effect is generally weaker than the hydrophobic effect, which is why large aggregates like WLMs (having N_{agg} > 1000) are usually not formed in polar solvents. In recent years, there has been renewed interest in studying self-assembly in nonaqueous media, including ionic liquids. One motivation to study polar solvents is that they can have freezing points (T_f) well below 0 °C. Recently, WLMs of a zwitterionic surfactant in water−EG mixtures were reported to exist at subzero temperatures.[26,27] However, self-assembly into WLMs under such extremely cold conditions has not been achieved in pure nonaqueous solvents, to our knowledge.

Here, we show that WLMs can indeed be formed in polar solvents like Gly and formamide if the surfactant and salt are carefully selected. Our surfactant of choice is a cationic surfactant with a long (C_{22}, unsaturated) tail (Figure 1C).[11−15] To form WLMs in solvents like Gly, this surfactant has to be combined with a salt having an organic counterion like sodium salicylate (NaSal) (Figure 1C). In addition to pure nonpolar solvents, we have also studied solvent mixtures, and in particular, mixtures of Gly and EG that have freezing points far below 0 °C. We have formed WLMs in these mixtures and find that the WLMs are preserved down to temperatures as low as −20 °C. The rheology of these WLMs under both steady and dynamic shear over a range of low temperatures extending into the subzero range is reported. In addition, the technique of small-angle neutron scattering (SANS) is used to probe the nanostructure of the WLMs at these temperatures. Our studies provide insights into the design rules for self-assembly in polar solvents as opposed to water. Apart from fundamental insights, our findings may also have technological importance. The ability to form WLMs and thereby convert a solvent into a viscoelastic fluid could be useful in a variety of scenarios. One possibility is as lubricants that can be stable under extremely low temperatures. Another possibility is as antifreeze liquids, which when sprayed onto airplane wings (or cars or wind turbines) would remain in place for a longer time due to their higher viscosity.[26]

EXPERIMENTAL SECTION

Materials. The following chemicals were obtained from Sigma-Aldrich: the surfactants CPyCl, cetyl trimethylammonium bromide (CTAB), and cetyl trimethyl ammonium *p*-toluene sulfonate (CTAT); the salts NaSal, NaTos, sodium chloride (NaCl), and potassium chloride (KCl); and the solvents Gly, EG, formamide, and propylene glycol. The surfactant EHAC was obtained from Akzo Nobel. For SANS experiments, deuterated Gly (d_8) was purchased from Cambridge Isotope Laboratories, and deuterated EG (d_4) was

DOI: 10.1021/acs.langmuir.9b02125
Langmuir 2019, 35, 12782−12791

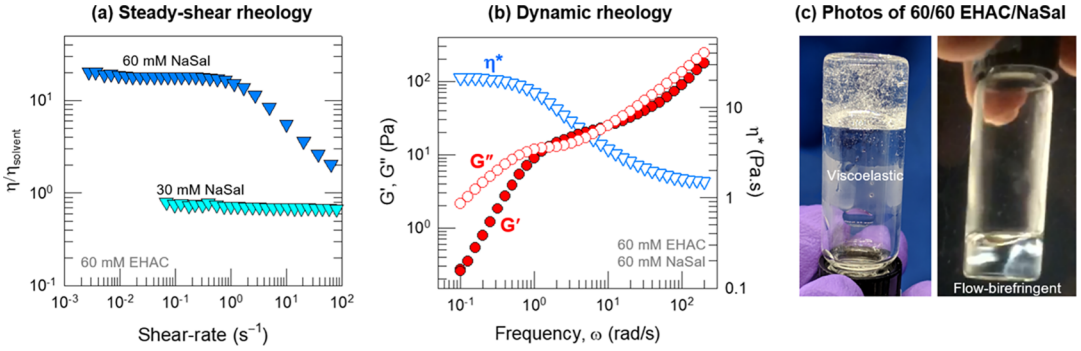

Figure 2. WLMs of EHAC−NaSal in Gly at 25 °C. (a) Steady-shear rheology (plots of the relative viscosity $\eta/\eta_{solvent}$ as a function of shear rate) for 60 mM EHAC samples containing 30 or 60 mM NaSal. (b) Dynamic rheology (plots of the elastic modulus G', viscous modulus G'', and complex viscosity η^* as functions of frequency ω) for the 60 mM EHAC + 60 mM NaSal sample. This sample shows shear thinning in steady shear and a viscoelastic response in dynamic rheology, indicating the presence of WLMs. (c) Visual observations further support this finding. The first photo shows that the sample is viscoelastic and is able to hold its weight in the inverted vial. The second photo, taken under crossed polarizers, shows that the sample is flow birefringent (streaks of light appear when the sample is shaken).

purchased from Polymer Source, Inc. The molecular structures of key surfactants and salts used in this study are shown in Figure 1C.

Sample Preparation. Stock solutions of the surfactants and salts were prepared by adding weighed amounts of each into the solvent of interest and heating to ∼60 °C on a hot plate under constant stirring for 4−5 h. After clear solutions were obtained, they were cooled and stored at room temperature. To prepare a sample with desired molar concentrations of surfactant and salt, the respective stock solutions were combined and diluted with the solvent. After vortex mixing, the sample was heated to 60 °C for 10−15 min and then cooled to room temperature. Samples were left at room temperature for at least a day before any measurements.

Rheology. Rheological experiments were conducted on an AR2000 stress-controlled rheometer (TA Instruments). A cone-and-plate geometry (2° cone) was used to perform the steady-shear and oscillatory-shear experiments. The temperature was controlled by a Peltier assembly on the rheometer, which employed a circulating fluid that was fed from a chiller. A 50/50 mixture of ethanol−water (with a T_f < −30 °C) was used as the circulating fluid. Rheological experiments were conducted at temperatures ranging from −5 to 65 °C. Dynamic rheology experiments were conducted in the linear viscoelastic regime for each sample, which was determined from strain-sweep experiments. For rheological experiments at temperatures below 0 °C, a crucial issue was the formation of ice on the cone-and-plate. To minimize ice formation, the plates were coated with EG, then wiped dry. This allowed experiments to be conducted down to −5 °C.

Small-Angle Neutron Scattering. SANS experiments were performed at the National Institute of Standards and Technology (NIST), Gaithersburg, MD, on the NG-B (30 m) beamline. Neutrons with a wavelength λ of 6 Å were selected and the range of wave vector q accessed was from 0.004 to 0.4 Å^{-1}. The sample holders were 1 mm titanium cells with quartz windows. The scattering data were reduced using IGOR-Pro software and were corrected to obtain an absolute scale of scattering intensity using NIST calibration standards. SANS fitting was done using the SasView software.

RESULTS AND DISCUSSION

Formation of WLMs in Glycerol. We first describe the formation of WLMs in Gly at 25 °C. Gly is a polar solvent that has high cohesive energy density (CED) and strong hydrogen-bonding capability.[3,33] Therefore, Gly can allow the self-assembly of micelles; however, previous reports of micelles in Gly have been confined to small micelles with low aggregation numbers.[33] We first attempted to form WLMs in Gly using the same precursors used previously to form WLMs in water. The vast majority of the studies on aqueous WLMs have been done with cationic surfactants, especially those with a C_{16} tail like CPyCl and CTAB.[6−8] To form WLMs, these surfactants are usually combined with either simple, inorganic salts (such as NaCl and KCl), or organic "binding" salts (such as NaSal and NaTos). We studied if any of these surfactant/salt combinations could result in WLMs in Gly. To initially assess the presence of WLMs, we resorted to visual inspection, looking for samples with high viscosities (as indicated by a gradual flow out of a vial or the persistence of bubbles). However, none of the above combinations yielded WLMs. CTAB was found to be insoluble in Gly at all concentrations at room temperature, consistent with previous studies.[39] CPyCl was soluble, but did not form WLMs with the salts tested (data on the viscosities of CPyCl/NaSal mixtures are presented later).

Next, we tried EHAC, a cationic surfactant with a longer C_{22} tail (see Figure 1C for structure). Because of its longer tail, EHAC is a much stronger surfactant than CTAB or CPyCl; for example, the critical micelle concentration of EHAC is about 50 times lower than that of the others.[11,12] WLMs of EHAC have been studied in water and can be induced both by simple and binding salts.[11−15] In Gly, though, we find that EHAC forms WLMs only when mixed with binding salts like NaSal. Figure 2 shows visual observations and rheological data at 25 °C for a sample containing 60 mM EHAC + 60 mM NaSal. This sample is highly viscous (Figure 2a) and viscoelastic (Figure 2b). Visual observations show that the sample flows slowly out of a tilted or inverted vial and that bubbles are trapped in the sample after it is shaken (Figure 2c). The sample also exhibits flow birefringence, which is a phenomenon associated with WLMs.[7] When a sample of WLMs is sheared (e.g., by shaking), the WLM chains align along the direction of shear, and as a result, the sample shows birefringence, i.e., it has different refractive indices along perpendicular directions. A simple way to see birefringence is by viewing the sample under crossed polarizer plates, whereupon streaks of light become visible in the sample when shaken (as can be noted in Figure 2c); these indicate aligned domains of WLMs. Note that there is no birefringence in the sample at rest because the WLM chains will not be aligned; rather they will be entangled into an isotropic network.[7]

The rheology of the 60 mM EHAC + 60 mM NaSal sample in Gly at 25 °C is consistent with the presence of WLMs. The steady-shear rheological data (Figure 2a) are shown as plots of

DOI: 10.1021/acs.langmuir.9b02125
Langmuir 2019, 35, 12782−12791

the relative viscosity, i.e., the ratio of sample viscosity with respect to solvent viscosity ($\eta/\eta_{solvent}$), as a function of shear rate. The 60 mM NaSal sample shows a constant and high viscosity at low shear rates (in the Newtonian plateau), with its zero-shear viscosity η_0 being about 20 times that of the solvent. The high η_0 indicates the presence of long, entangled WLMs.[7,8] Above a critical shear-rate, η drops with increasing shear, indicating a shear-thinning response. Shear-thinning arises because the WLM chains tend to align with the flow.[8] For comparison, data are also shown in Figure 2a for a sample of 60 mM EHAC + 30 mM NaSal. This sample has the same viscosity as that of the solvent, i.e., there is no thickening, which implies that the micelles in it are not WLMs, but short cylinders. Long WLMs are only seen around an equimolar ratio of EHAC to NaSal, as will be further clarified in Figure 3.

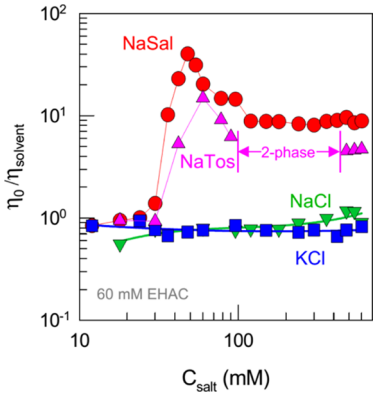

Figure 3. Effects of different salts on the formation of WLMs by EHAC in glycerol at 25 °C. The plot shows the relative zero-shear viscosity ($\eta_0/\eta_{solvent}$) as functions of salt concentration for various salts, with the EHAC concentration fixed at 60 mM. WLM formation is reflected by a substantial increase in η_0 and is observed only with NaSal and NaTos.

The dynamic rheology of the 60 mM EHAC + 60 mM NaSal sample also reveals interesting features (Figure 2b). The elastic modulus G' and the viscous modulus G'' are both strong functions of the frequency ω, and the data overall reflect a viscoelastic response, consistent with the presence of a WLM network.[7,8] However, typical WLMs in water show a single intersection of G' and G'' at a crossover frequency ω_c.[6,7] The relaxation time t_R of the WLMs is then given by $1/\omega_c$. Here, the Gly-based WLMs show two intersection points of G' and G'' over the frequency range. At low ω, a "terminal" region occurs, as expected, where $G'' > G'$, indicative of viscous behavior. Thereafter, at intermediate ω (1 to 10 rad/s), G' overtakes G'', indicating a transition to an elastic response at short timescales. Usually, G' will then become ω-independent and reach a plateau value, termed the plateau modulus G_p, which correlates with the mesh size of the entangled WLM network.[6] Here, instead, G' shows an upturn at $\omega > 10$ rad/s and at these short timescales, we again find that $G'' > G'$, indicating viscous dissipation. To our knowledge, such a rheological response has never been reported before for WLMs!

We have also plotted the complex viscosity η^* as a function of ω in Figure 2b. $\eta^*$is a quantity derived from G' and G'', as per eq 1[40,41]

$$\eta^* = \frac{\sqrt{G'^2 + G''^2}}{\omega} \quad (1)$$

Although the complex viscosity η^* is comparable to the viscosity η from steady shear, we note that the η^* curve in Figure 2b shows two plateaus, one at low ω and the other at high ω. In contrast, η shows one plateau at low shear rates and then a monotonic decrease at higher shear rates. The presence of two plateaus in η^* versus ω is again unusual for WLMs, and it also has never been reported previously.[7,8] Why is the rheology different for WLMs in Gly compared to those in water? This is a complex topic, which we will address in detail in a separate paper. Briefly, we believe there are two reasons for the differences: first, the structure of the WLMs in the two solvents, and second, the differences between the solvents themselves (i.e., the fact that water has a low viscosity compared to Gly). For the rest of this paper, we will focus on the physical chemistry of the WLMs in Gly as a function of salt, surfactant, and temperature.

Effects of Salt Concentration and Type. Figure 3 shows the relative zero-shear viscosity $\eta_0/\eta_{solvent}$ of glycerol solutions with 60 mM EHAC and increasing concentrations (C_{salt}) of different salts. The η_0 for each sample is obtained from the Newtonian plateau at low shear rates in the steady-shear data (similar to the curves shown in Figure 2a). In the case of NaSal, there is no increase in viscosity until C_{NaSal} = 36 mM (i.e., molar ratio C_{NaSal}/C_{EHAC} = 0.6), indicating that there is no growth of WLMs up to this point. Thereafter, the viscosity increases with increasing C_{NaSal} and reaches a peak at C_{NaSal} = 48 mM (C_{NaSal}/C_{EHAC} = 0.8). The viscosity peak occurs close to the equimolar ratio of salt/surfactant, which suggests that there is molecular binding of the two species. Beyond the equimolar ratio, further addition of NaSal causes the viscosity to decrease and finally reaches a plateau. Note that the peak value of η_0 is 34 Pa s, which is comparable to the η_0 values exhibited by aqueous WLMs at similar surfactant and salt concentrations.[7,8] However, since Gly is a viscous solvent, the peak enhancement in Gly viscosity due to the WLMs is only a factor of about 40.

Similar results as those for NaSal are shown in Figure 3 for a second binding salt, NaTos (structure in Figure 1B). Again, there is a sharp increase in viscosity of 60 mM EHAC solutions around C_{NaTos} = 36 mM, indicating growth of WLMs. The peak in η_0 is reached at C_{NaTos} = 60 mM (C_{NaTos}/C_{EHAC} = 1) and the value of η_0 at this peak is 13 Pa s. With further increase in C_{NaTos}, the viscosity drops to a plateau. Note that, between 90 and 480 mM NaTos, EHAC/NaTos samples in Gly at 25 °C separate into two coexisting liquid phases, which is why no data are shown for the viscosities over this concentration range. The two phases are a coacervate phase that contains most of the surfactant and a thin salt solution. Photos of selected samples are shown in Figure S1 (Supporting Information). Such "coacervation" is unusual for surfactant solutions, but interestingly, it also occurs for EHAC/NaTos mixtures in water at 25 °C.[12] In contrast to NaSal and NaTos, simple salts such as NaCl and KCl do not induce any appreciable change in solution viscosity, regardless of the salt concentration (Figure 3). We conclude that simple salts are incapable of inducing WLMs of cationic surfactants in Gly (and the same is true in other polar solvents).

We have also evaluated a variety of surfactants for their ability to form WLMs in Gly. As mentioned, CTAB has limited solubility in Gly, and this is also the case for other alkyl-TABs

DOI: 10.1021/acs.langmuir.9b02125
Langmuir 2019, 35, 12782−12791

with C_{14} or C_{12} tail.[33] Another widely used cationic surfactant in WLM studies is CTAT,[42] but this is also insoluble in Gly. The one cationic surfactant that was reasonably soluble in Gly was CPyCl. Figure 4 shows the viscosities of 60 mM CPyCl

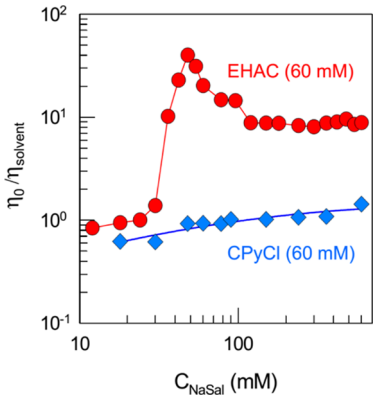

Figure 4. Comparison of EHAC and CPyCl for their ability to form WLMs in glycerol at 25 °C. The plot shows the relative zero-shear viscosity ($\eta_0/\eta_{solvent}$) as functions of NaSal concentration for the two surfactants, with the surfactant concentration held constant at 60 mM. WLM formation is reflected by a substantial increase in η_0 and is observed only with EHAC.

solutions in Gly as a function of NaSal. Negligible increases in viscosity are seen up to 600 mM NaSal, indicating a lack of WLMs. Thus, CPyCl/NaSal mixtures do not form WLMs in Gly, although they do so in water. In contrast, EHAC/NaSal mixtures give rise to WLMs in both Gly and water. The inability of CPyCl to form WLMs in Gly suggests that its shorter tail (C_{16}) is insufficient to induce extensive self-assembly in nonaqueous systems.

A summary of the results thus far is sketched in Figure 5. To form WLMs in Gly, both a long-tailed surfactant like EHAC and a binding salt like NaSal or NaTos are required. All other combinations of surfactants and salts failed to produce WLMs. Why are there differences between simple and binding salts in Gly? In water, both kinds of salts induce WLMs, but by different mechanisms. It is helpful to relate salt effects to the critical packing parameter (CPP) = a_{tail}/a_{hg}, where a_{tail} and a_{hg} refer to the average cross-sectional areas of the tail and the headgroup, respectively.[2,3] For a cationic surfactant in water, the CPP will be ∼1/3 and the molecule will have a cone shape (Figure 5). This is because the headgroups, when ionized, will experience significant electrostatic repulsions with each other, and thus the effective a_{hg} will be large relative to a_{tail}.[2,3] Molecules with a CPP of 1/3 will tend to form spherical micelles.

When a salt like NaCl is added to the water, the ions will screen the electrostatic repulsions, reducing a_{hg} and thereby increasing the CPP from 1/3 to 1/2. This change in CPP causes a transition from spherical to cylindrical micelles (and thereby, eventually, to WLMs). Thus, simple salts induce micellar growth, not by binding to micelles, but by screening the micellar charge.[8,11] Binding salts like NaSal, on the other hand, have aromatic counterions that are significantly hydrophobic.[8,43] These counterions will penetrate the palisade layer of the micelles and embed in the hydrophobic core (Figure 5).[43] At the same time, the anionic (e.g., carboxylate) moiety of the counterion will bind to the cationic headgroups. Because of this binding, the micellar charge will be appreciably reduced, and in turn, the repulsions will be lowered. Thus, once again, an increase in CPP from 1/3 to 1/2 will occur, causing a sphere-to-cylinder (WLM) transition.[7,8] If all the counterions were to bind to the micelles, the net charge on the micelles would be lowest at an equimolar ratio of salt/surfactant.

Our results suggest that the binding of counterions like salicylate and tosylate to EHAC micelles occurs quite readily in a polar solvent like Gly, which explains the growth of WLMs. This is illustrated in Figure 5. Presumably, the solvophobic effect with Gly is sufficiently strong to allow the counterions to insert their aromatic ring into the micellar core. One indication of such binding is the fact that the viscosity maxima occur at or near the equimolar ratio of salt/surfactant. However, simple salts like NaCl seem ineffective at screening the electrostatic repulsions between EHAC headgroups in Gly. The reason for this is not completely clear at the moment. It is possible that

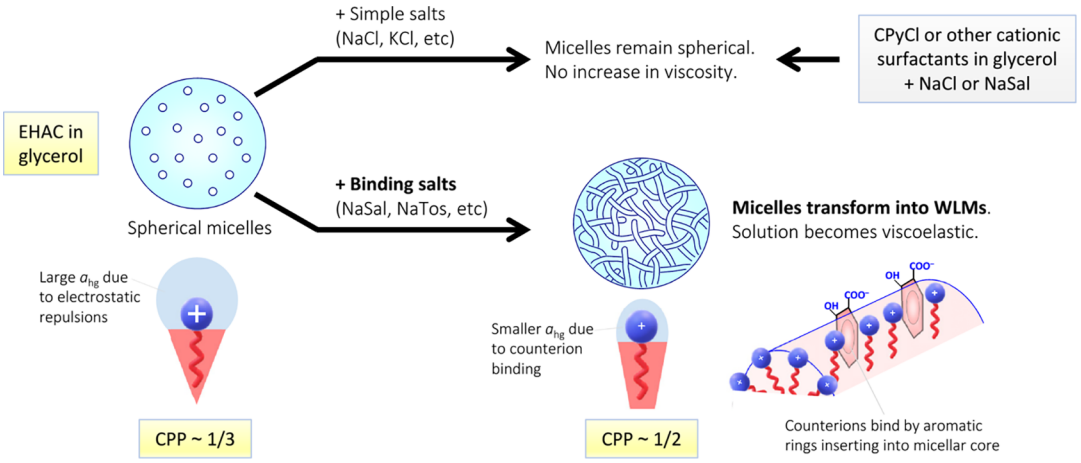

Figure 5. Conditions for WLM formation in polar solvents like glycerol and a mechanistic picture for the same. WLMs form only when EHAC is combined with binding salts like NaSal or NaTos. For all other cases (EHAC + simple salts; other surfactants + any salts), no WLMs are produced. In the absence of salt, EHAC has a critical packing parameter (CPP) of ∼1/3 because of strong electrostatic repulsions between its headgroups (and thereby a large area per headgroup a_{hg}). When a binding salt like NaSal is added, its counterions will bind to EHAC micelles. This will occur with the aromatic rings inserting into the hydrophobic core of the micelle. The anionic counterions, in turn, will neutralize the cationic headgroups and thus reduce a_{hg}, which increases the CPP to ∼1/2. This will induce the spherical micelles to transform into WLMs.

DOI: 10.1021/acs.langmuir.9b02125
Langmuir 2019, 35, 12782−12791

these salts do not completely dissociate into ions in Gly due to its lower dielectric constant compared to that of water (see Table 1). Alternately, electrostatic screening by ions may not be as effective in Gly compared to water. This aspect requires further study.

Table 1. Selected Properties of Various Polar Solvents Compared with Those of Water

solvent	dielectric constant ε (at 20 °C)	surface tension γ (mN/m) (at 20 °C)	freezing point T_f (°C)	Gordon parameter G (J mol$^{1/3}$ m^{-3})
water	80	72.8	0	2.74
glycerol	47	64.0	18	1.52
formamide	109	58.2	3	1.73
ethylene glycol	37	47.7	−13	1.36

WLMs in Other Polar Solvents. Having identified the EHAC/NaSal system as one that results in WLMs in Gly, we proceeded to study if WLMs could be formed by the same surfactant/salt combination in other polar solvents. For a polar solvent to allow self-assembly through the solvophobic effect, it must have a high CED, i.e., there must be strong interactions between the solvent molecules. Solvents with high CED tend to be highly polar (as quantified by their dielectric constant ε) and also have strong hydrogen-bonding ability.[36−39] One way to quantify the CED is by the Gordon parameter G, which is given by[3]

$$G = \frac{\gamma}{(V_s^{mol})^{1/3}} \quad (2)$$

where γ is the surface tension of the solvent and V_s^{mol} is its molar volume. Table 1 lists ε, γ, G, and also the freezing point T_f for a few solvents in which self-assembly has been studied previously. Water has the highest values of G and γ and is thus the most favorable solvent for self-assembly. Gly, formamide, and EG are three other solvents with high G. Note that formamide also has the highest ε. Although Gly has lower G and ε than formamide and water, it has strong hydrogen-bonding capability through its three hydroxyl groups. We have already demonstrated the formation of WLMs in Gly. Thus, we proceeded to try the other solvents in this table.

One further aspect to consider at this stage is the effect of temperature on self-assembly. Generally, self-assembly becomes stronger at lower temperatures,[1,2] and WLMs are a case in point. The contour (end-to-end) length L of WLMs increases exponentially with decreasing absolute temperature T, as per the following equation[6,11]

$$L \approx \sqrt{\phi} \cdot \exp(E_c/2k_BT) \quad (3)$$

where k_B is Boltzmann's constant, ϕ is the volume fraction of the WLMs, and E_c is their end-cap energy. The key parameter here is E_c, which is the energy penalty associated with surfactant molecules that are stuck in the hemispherical end-caps of the WLMs rather than in their cylindrical bodies. The higher the E_c, the longer the WLMs will grow (to avoid forming end-caps).[6,11] As T is decreased, the exchange of surfactants between micelles is slowed down; this mitigates the influence of the end-caps and thereby allows the chains to grow longer. Longer WLMs will take a longer time to relax, and in turn, the solution will become more viscous. Based on eq 3, even if the WLMs are not very long at room temperature, they could become much longer upon cooling. For this reason, we have extended our studies on WLM formation in the solvents from Table 1 to temperatures well below room temperature.

It should be noted that studies on WLMs in water have rarely been conducted at temperatures much below 25 °C. The reason for this lies in a key characteristic of surfactants called their Krafft temperature T_K.[1] This is the temperature below which the surfactant crystallizes out of solution, and hence, no micelles can be formed below T_K. Generally, T_K increases with the surfactant tail length:[1,18] it is ∼20 °C for surfactants with saturated C_{16} tails, such as CTAB and CPyCl, and it is above room temperature if the tail is saturated-C_{18} or longer. Thus, the relatively high T_K values of CTAB and CPyCl have posed a limitation to studying their WLMs at low temperatures. In the case of EHAC, the erucyl tail has a cis-unsaturation in its middle (Figure 1B), and this represents a kink or bend in the tail. Due to this kink, EHAC molecules cannot pack tightly into a crystal, which is why EHAC has a very low T_K (<−20 °C).[11,12] Thus, our choice of EHAC as the surfactant allows us to investigate WLMs down to low temperatures.

Figure 6 shows representative data from steady-shear rheology on samples in different solvents. All samples have

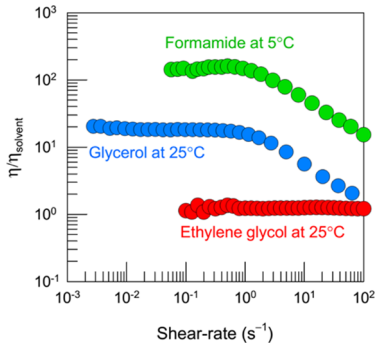

Figure 6. Steady-shear rheology of EHAC−NaSal samples in various solvents. The data are for the relative viscosity $\eta/\eta_{solvent}$ as a function of shear rate. All samples contain 60 mM EHAC. The NaSal concentration is 60 mM in the Gly sample and 90 mM in the formamide sample. Data are shown for Gly and EG at 25 °C and for formamide at 5 °C.

60 mM EHAC, whereas the NaSal is 60 or 90 mM. The data are for the relative viscosity ($\eta/\eta_{solvent}$) as a function of shear rate. In EG at 25 °C, there is no increase in viscosity and the sample shows Newtonian behavior, indicating a lack of WLMs. Similar data were obtained in EG at lower temperatures, regardless of the EHAC or NaSal content. In formamide at 25 °C, the sample exhibited $\eta/\eta_{solvent}$ close to 1 and the behavior was Newtonian. However, at lower temperatures, the rheology became characteristic of WLMs. Data at 5 °C are provided in Figure 6 and data at different temperatures are included in Figure S2 in the Supporting Information. The plot in Figure 6 clearly shows a profile similar to that for Gly: that is, there is a high η_0 at low shear rates and shear thinning at higher shear rates. This implies the presence of long, entangled WLMs of EHAC/NaSal in formamide. Note that η_0 for this sample is about 200 times that of the solvent at 5 °C, which is a substantial enhancement in viscosity.

WLMs at Low and Subzero Temperatures. Next, we attempted to push the limits of WLM formation to temperatures below 0 °C. One way to obtain a liquid with a low freezing temperature T_f is by mixing pure solvents. For

DOI: 10.1021/acs.langmuir.9b02125
Langmuir 2019, 35, 12782−12791

example, it is well known that mixtures of Gly and water have lower T_f than either of the pure liquids.[44] In a similar vein, we studied mixtures of Gly and EG. As shown in Table 1, the T_f for Gly is 18 °C and that for EG is −13 °C. We confirmed that Gly−EG mixtures over a vast composition range have lower T_f than those of the individual solvents (see Figure S3 in the Supporting Information). For our studies, we used a 90/10 mixture of Gly−EG, which has a T_f < −5 °C. To form WLMs in this mixed solvent, we added 60 mM EHAC + 120 mM NaSal. Although WLMs did not form in pure EG at this composition, they did so in the 90/10 Gly−EG mixture. Through visual observations, we confirmed that the sample remained clear and viscoelastic even when cooled to temperatures as low as −20 °C.

Figure 7 shows steady-shear rheological data on the above sample over a temperature range from −5 to 35 °C. At all

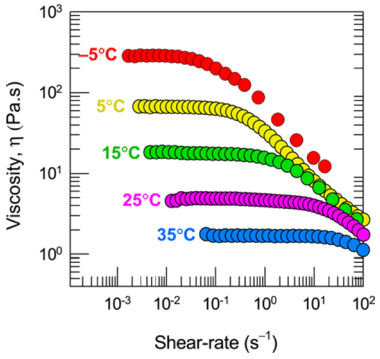

Figure 7. Steady-shear rheology of WLMs in a low-freezing solvent (90/10 mixture of Gly−EG) from ambient to subzero temperatures. The data are for the viscosity η as a function of shear rate. The sample contains 60 mM EHAC and 120 mM NaSal.

temperatures, the sample shows a shear-thinning response similar to that in Figure 2a; thus the data reflect the presence of WLMs over the temperature range. The zero-shear viscosity η_0 increases significantly with decreasing temperature: η_0 is 1.7 Pa s at 35 °C and 285 Pa s at −5 °C, that is, there is a 150-fold increase in η_0 over a 40 °C span. At even lower temperatures, the viscosity increases further and the sample becomes almost gel-like, but we could not perform accurate measurements due to experimental limitations; hence, data are not shown. Still, Figure 7 is significant because it shows systematic rheological data on WLMs at temperatures below 0 °C.

The increase in zero-shear viscosity η_0 of WLMs with decreasing temperature is expected to follow an exponential relation[6,11]

$$\eta_0 = A \cdot \exp(E_a/RT) \quad (4)$$

where A is a pre-exponential factor, T the absolute temperature, and E_a the flow activation energy. This relationship arises from the exponential rise in WLM contour length L with decreasing T, as given in eq 3. That is, the longer the WLMs, the higher the η_0. To verify if eq 4 holds for our system, we construct a semilog (Arrhenius) plot of η_0 versus $1/T$. This is shown in Figure 8, and the data fall on a straight line, as expected. From the slope, we calculate the flow activation energy E_a to be 88 kJ/mol for this sample. For comparison, WLMs of 60 mM EHAC + 30 mM NaSal in water had a much higher E_a of 198 kJ/mol. At first glance, this suggests that E_a may be higher for WLMs in water. However, WLMs based on

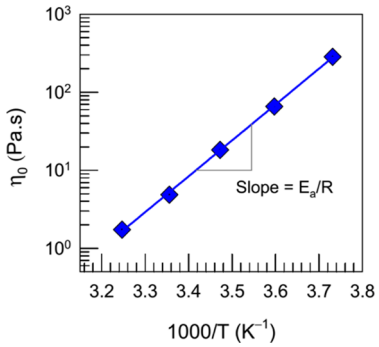

Figure 8. Arrhenius (semilog) plot of the zero-shear viscosity vs $1/T$, using the data from Figure 7. The sample contains 60 mM EHAC and 120 mM NaSal in a 90/10 Gly−EG mixture.

other surfactant/salt combinations in water have been reported to show similar E_a values to those determined here.[13,14,16]

Nanostructure from SANS. Thus far, we have provided evidence from rheology and visual observations for the presence of WLMs in polar liquids. To further confirm the nanostructure, we resorted to SANS. Samples for SANS were prepared using deuterated solvents to ensure that there was sufficient contrast between the scattering objects and the continuous phase. SANS data are provided in Figure 9 as plots of the scattering intensity I versus wave vector q. In Figure 9a, data are shown at 25 °C for samples containing 60/30 and 60/60 EHAC/NaSal in Gly. There is an upturn (higher slope) for I at low q for the 60/60 sample compared to the 60/30 one. This is consistent with the presence of longer micelles (WLMs) in the former, and it also tallies with the higher viscosities of the former from Figure 3. For comparison purposes, a slope of −1 on the log−log plot is marked on all the plots; this corresponds to the scaling relationship expected from theory for scattering from long, noninteracting cylinders ($I \sim q^{-1}$).[45,46] The slope of I in the low-q limit for the 60/60 sample is −0.7, which is close to −1. Both samples show nearly identical data at intermediate and high q, which suggests that both contain cylindrical micelles with similar radii (estimated to be around 2.4 nm; see below), but different lengths.

Next, the scattering from the 60/30 EHAC/NaSal sample in Gly is studied at a higher temperature of 65 °C. In this case (Figure 9b), I reaches a plateau at low q, which means that the micelles present are spherical. Note that the same sample at 25 °C shows a much higher intensity at low q with a low-q slope of −0.3. The implication is that the relatively short cylinders present in this sample at 25 °C shorten further and become nearly spherical at 65 °C. Taken together, Figures 9a and 9b provide structural evidence for the effects of composition and temperature on EHAC self-assembly in Gly. The data confirm that: (a) micelles are present; (b) the micelles grow with addition of NaSal; (c) the micelles are likely to be long cylinders (WLMs) at an equimolar ratio of salt/surfactant at 25 °C; and (d) increasing temperature shortens the micelles. We should emphasize that the above SANS data are very similar to those reported previously for aqueous WLMs, including those of EHAC/NaSal.[12,15,17]

We also conducted SANS studies using the 90/10 mixture of Gly−EG (both deuterated), corresponding to Figure 7. Data for a sample of 60/60 EHAC/NaSal in this solvent mixture are shown over a temperature range from −20 to 80 °C in Figure 9c. Over the entire range, the data overlap at high q, which suggest that micelles with comparable radii are present at all

DOI: 10.1021/acs.langmuir.9b02125
Langmuir 2019, 35, 12782−12791

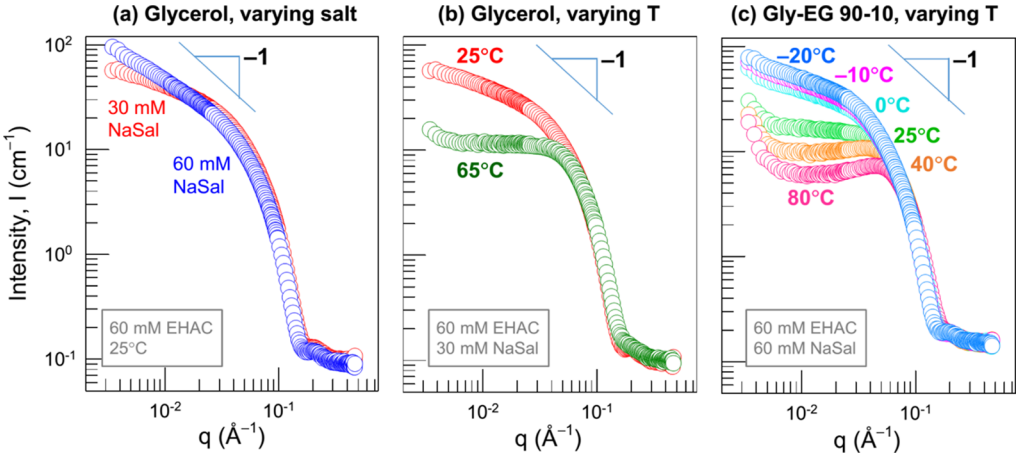

Figure 9. SANS plots for samples of EHAC/NaSal in deuterated solvents. Each plot shows the scattered intensity I vs wave vector q. (a) Data for 60/30 and 60/60 mM EHAC/NaSal in Gly at 25 °C. (b) Data for 60/30 EHAC/NaSal in Gly at 25 and 65 °C. (c) Data for 60/60 EHAC/NaSal in 90/10 Gly−EG at temperatures ranging from −20 to 80 °C.

temperatures. At the lowest temperatures, there is increased scattering at low q and the slope of I at low q becomes approximately −0.4. This is again indicative of micellar growth into cylinders (WLMs). As temperature is increased, the intensity drops at low and intermediate q, implying a reduction in the cylinder length. An unusual upturn in intensity is observed at low q in the 40 and 80 °C data. Such an upturn generally suggests that there are attractive interactions between the scattering objects,[46] although it is not clear why that should arise in this sample. The upturn is much more pronounced for the 90/10 Gly−EG sample in Figure 9c than for the Gly sample in Figure 9b. If the upturn is ignored, the conclusion to be drawn from Figure 9c would be similar to the one from above: i.e., that the micelles shorten upon heating, or conversely lengthen (into WLMs) upon cooling.

SANS data can generally be fit to models, from which the sizes of scatterers can be extracted.[45,46] We have performed such model fitting, and the details are provided in the Supporting Information (Figure S5 and the accompanying text). Excellent fits are obtained for a model that incorporates the form factor for cylinders of radius R and length L along with the structure factor for hard spheres.[45] The values of key parameters in the model are shown in Table S1 in the Supporting Information. The micellar radius R is ∼2.4 nm, and this is reliably obtained from the model fits. In fact, the same R can be calculated in a model-independent manner by plotting the scattering data in a cross-sectional Guinier plot, i.e., a plot of $\ln(Iq)$ versus q^2.[46]

With regard to the model fits in Figure S5, we believe there is need for caution in interpreting some of the parameters obtained from the modeling. Specifically, the models are rather insensitive to the micellar contour length L, and hence L cannot be accurately obtained from these fits. The underlying reason is that WLMs are expected to have contour lengths L exceeding 100 nm. SANS, on the other hand, provides an accurate window primarily into structures between about 0.2−30 nm. In effect, when the WLM length exceeds this window, SANS only probes a portion of the entire WLM chain and is therefore insensitive to the contour length.[46] For example, the SANS data in Figure 9c for WLMs at temperatures of 0 and −20 °C are nearly identical; however, from the rheology data, we know that at the colder temperature, the WLMs must be much longer, which is why the sample is much more viscous. Despite these issues, it is clear that the SANS modeling supports the presence of surfactant-based WLMs in polar solvents.

Another model-independent approach to SANS analysis is by use of the Indirect Fourier Transform (IFT) method,[47,48] which permits the data to be analyzed without making a priori assumptions about the shapes or sizes of the scatterers. Figure S6 shows the pair distance distribution functions $p(r)$ obtained from IFT analysis of the SANS data from the 60/60 EHAC/NaSal sample at 25 and 65 °C. The $p(r)$ at 25 °C is asymmetrical and the curve hits the x-axis at around 15 nm. This shape of $p(r)$ is known to be characteristic of cylindrical micelles,[47,48] with 15 nm being a lower estimate for their length. On the other hand, the $p(r)$ at 65 °C is symmetrical and this shape is characteristic of spherical micelles.[47,48] In this case, the point where $p(r)$ hits the x-axis is about 7 nm, which corresponds to the diameter of the spheres. Thus, the IFT analysis also suggests that the micelles are larger and cylindrical (i.e., WLMs) at low temperatures and smaller and spherical at high temperatures, which is consistent with the discussion above.

■ CONCLUSIONS AND OUTLOOK

We have shown that it is possible for surfactants to self-assemble into large aggregates, specifically WLMs, in polar solvents like Gly and formamide. This was achieved by combining a long-tailed (C_{22}) cationic surfactant (EHAC) with a "binding" salt (NaSal or NaTos). Simple salts (NaCl or KCl) were unable to induce EHAC to form WLMs in polar solvents, although they are able to do so in water. Also, shorter-tailed (C_{16}) cationic surfactants did not assemble into WLMs in these solvents, whether they were combined with binding or simple salts. Thus, both the surfactant and the salt have to be chosen carefully to enable WLM formation in these non-aqueous systems. WLMs in polar solvents display viscoelastic and shear-thinning rheology, much like WLMs in water. However, the dynamic rheology of the former is quite unusual—the frequency spectra reveal multiple intersections of the elastic and viscous moduli (G' and G''). We have exploited the low Krafft point of EHAC and the low freezing points of Gly−EG mixtures to devise formulations in which WLMs persist down to subzero temperatures (−20 °C). SANS measurements confirm that WLMs are still present at these low

DOI: 10.1021/acs.langmuir.9b02125
Langmuir 2019, 35, 12782−12791

temperatures. Thereby, we have been able to extend the range for WLM formation to much lower temperatures than in previous studies.

The ability to create nonaqueous viscoelastic fluids that withstand low temperatures is one notable point of this study. Because the fluids are formed by mixing commonly available precursors, they could be prepared in large quantities at low cost. Thereby, the fluids would be suitable for industrial applications that require cold temperatures, including as lubricants or as antifreeze coatings on the surfaces.[26] A simple experiment to illustrate the utility is shown in Figure S4 of the Supporting Information. Here, aluminum-covered surfaces are placed at a near-vertical angle, and a given amount of fluid is introduced onto it. As an example of a low-freezing liquid, we employ a 90/10 Gly−EG mixture (same as in Figure 7). If the liquid alone is introduced onto the surface, it flows down and dewets the surface in a short time, leaving it exposed (Figure S4a). However, if the same Gly−EG with WLMs of EHAC/NaSal is introduced, it too flows down, but still maintains a thin film over the entire surface (Figure S4b). Note that this is not just because the fluid has a higher viscosity, rather it reflects the viscoelasticity of the WLM solution. In fact, due to the shear-thinning nature of WLMs, the viscosity at high shear rates (that are commonly encountered in spraying or blading operations) will be close to that of the solvent (see Figure 7). Thus, spraying such viscoelastic fluids onto a surface such as aircraft wings can be readily accomplished, and the fluids could be highly effective for de-icing or lubrication applications.

■ ASSOCIATED CONTENT

Supporting Information

The Supporting Information is available free of charge on the ACS Publications website at DOI: 10.1021/acs.langmuir.9b02125.

Additional rheological data on certain samples, data on the properties of solvent mixtures, further analysis of SANS spectra, and data showing the suitability of these fluids for coating surfaces (PDF)

■ AUTHOR INFORMATION

Corresponding Authors

*E-mail: sraghava@umd.edu (S.R.R.).
*E-mail: yjfeng@scu.edu.cn (Y.F.).

ORCID

Yujun Feng: 0000-0001-5046-6085
Srinivasa R. Raghavan: 0000-0003-0710-9845

Notes

The authors declare no competing financial interest.

■ ACKNOWLEDGMENTS

This work was partially supported by a grant from the NIST Center for Neutron Research (NCNR). We also thank the NCNR for facilitating the SANS experiments performed as part of this work. We acknowledge the following lab members for their assistance in performing some of the experiments: Jane Njihia, Kerry DeMella, Sohyun Ahn, Leah Borden, Hema Choudhary, Nikhil Subraveti and Ben Thompson.

■ REFERENCES

(1) Jonsson, B.; Lindman, B.; Holmberg, K.; Kronberg, B. *Surfactants and Polymers in Aqueous Solutions*; Wiley: New York, 1998.

(2) Evans, D. F.; Wennerstrom, H. *The Colloidal Domain: Where Physics, Chemistry, Biology, and Technology Meet*; Wiley-VCH: New York, 2001.

(3) Israelachvili, J. N. *Intermolecular and Surface Forces*, 3rd ed.; Academic Press: San Diego, 2011.

(4) *Giant Micelles: Properties and Applications*; Zana, R., Kaler, E. W., Eds.; CRC Press: Boca Raton, 2007.

(5) *Wormlike Micelles: Advances in Systems, Characterisation and Applications*; Dreiss, C. A., Feng, Y. J., Eds.; RSC: Cambridge, 2017.

(6) Cates, M. E.; Candau, S. J. Statics and dynamics of worm-like surfactant micelles. *J. Phys.: Condens. Matter* **1990**, *2*, 6869−6892.

(7) Rehage, H.; Hoffmann, H. Viscoelastic surfactant solutions - Model systems for rheological research. *Mol. Phys.* **1991**, *74*, 933−973.

(8) Dreiss, C. A. Wormlike micelles: where do we stand? Recent developments, linear rheology and scattering techniques. *Soft Matter* **2007**, *3*, 956−970.

(9) Yang, J. Viscoelastic wormlike micelles and their applications. *Curr. Opin. Colloid Interface Sci.* **2002**, *7*, 276−281.

(10) Sullivan, P.; Nelson, E. B.; Anderson, V.; Hughes, T. Oilfield Applications of Giant Micelles. In *Giant Micelles: Properties and Applications*; Zana, R., Kaler, E. W., Eds.; CRC Press: Boca Raton, 2007; pp 453−472.

(11) Raghavan, S. R.; Kaler, E. W. Highly viscoelastic wormlike micellar solutions formed by cationic surfactants with long unsaturated tails. *Langmuir* **2001**, *17*, 300−306.

(12) Raghavan, S. R.; Edlund, H.; Kaler, E. W. Cloud-point phenomena in wormlike micellar systems containing cationic surfactant and salt. *Langmuir* **2002**, *18*, 1056−1064.

(13) Croce, V.; Cosgrove, T.; Maitland, G.; Hughes, T.; Karlsson, G. Rheology, cryogenic transmission electron spectroscopy, and small-angle neutron scattering of highly viscoelastic wormlike micellar solutions. *Langmuir* **2003**, *19*, 8536−8541.

(14) Couillet, I.; Hughes, T.; Maitland, G.; Candau, F.; Candau, S. J. Growth and scission energy of wormlike micelles formed by a cationic surfactant with long unsaturated tails. *Langmuir* **2004**, *20*, 9541−9550.

(15) Kalur, G. C.; Frounfelker, B. D.; Cipriano, B. H.; Norman, A. I.; Raghavan, S. R. Viscosity increase with temperature in cationic surfactant solutions due to the growth of wormlike micelles. *Langmuir* **2005**, *21*, 10998−11004.

(16) Kalur, G. C.; Raghavan, S. R. Anionic wormlike micellar fluids that display cloud points: Rheology and phase behavior. *J. Phys. Chem. B* **2005**, *109*, 8599−8604.

(17) Kumar, R.; Kalur, G. C.; Ziserman, L.; Danino, D.; Raghavan, S. R. Wormlike micelles of a C22-tailed zwitterionic betaine surfactant: From viscoelastic solutions to elastic gels. *Langmuir* **2007**, *23*, 12849−12856.

(18) Wang, Y.; Zhang, Y.; Liu, X.; Wang, J.; Wei, L.; Feng, Y. Effect of a hydrophilic head group on Krafft temperature, surface activities and rheological behaviors of erucyl amidobetaines. *J. Surfactants Deterg.* **2014**, *17*, 295−301.

(19) Kelleppan, V. T.; Moore, J. E.; McCoy, T. M.; Sokolova, A. V.; de Campo, L.; Wilkinson, B. L.; Tabor, R. F. Self-assembly of long-chain betaine surfactants: Effect of tailgroup structure on wormlike micelle formation. *Langmuir* **2018**, *34*, 970−977.

(20) Scartazzini, R.; Luisi, P. L. Organogels from lecithins. *J. Phys. Chem.* **1988**, *92*, 829−833.

(21) Shchipunov, Y. A. Lecithin organogel. *Colloids Surf., A* **2001**, *183-185*, 541−554.

(22) Tung, S.-H.; Huang, Y.-E.; Raghavan, S. R. A new reverse wormlike micellar system: Mixtures of bile salt and lecithin in organic liquids. *J. Am. Chem. Soc.* **2006**, *128*, 5751−5756.

(23) Liu, H.; Wang, W.; Yin, H.; Feng, Y. Solvent-Driven Formation of Worm-Like Micelles Assembled from a CO2-Responsive Triblock Copolymer. *Langmuir* **2015**, *31*, 8756−8763.

(24) Wei, Y.; Han, Y.; Zhou, H.; Wang, H.; Mei, Y. Rheological investigation of wormlike micelles based on gemini surfactant in EG-water solution. *J. Surfactants Deterg.* **2016**, *19*, 925−932.

DOI: 10.1021/acs.langmuir.9b02125
Langmuir 2019, 35, 12782−12791

(25) Zhou, H.; Han, Y.; Wei, Y.; Wang, H.; Mei, Y. Effect of EG and low temperature on solution behaviors of wormlike micelles. *J. Mol. Liq.* **2016**, *221*, 603−607.
(26) Yin, H.; Feng, Y.; Li, P.; Doutch, J.; Han, Y.; Mei, Y. Cryogenic wormlike micelles. *Soft Matter* **2019**, *15*, 2511−2516.
(27) Yin, H.; Feng, Y.; Li, P.; Doutch, J.; Han, Y.; Mei, Y. Cryogenic viscoelastic surfactant fluids: Fabrication and application in a subzero environment. *J. Colloid Interface Sci.* **2019**, *551*, 89−100.
(28) Ray, A. Micelle formation in pure ethylene glycol. *J. Am. Chem. Soc.* **1969**, *91*, 6511−6512.
(29) Evans, D. F.; Yamauchi, A.; Roman, R.; Casassa, E. Z. Micelle formation in ethylammonium nitrate, a low-melting fused salt. *J. Colloid Interface Sci.* **1982**, *88*, 89−96.
(30) Wârnheim, T. Aggregation of surfactants in nonaqueous, polar solvents. *Curr. Opin. Colloid Interface Sci.* **1997**, *2*, 472−477.
(31) Aramaki, K.; Olsson, U.; Yamaguchi, Y.; Kunieda, H. Effect of Water-Soluble Alcohols on Surfactant Aggregation in the C12EO8-System. *Langmuir* **1999**, *15*, 6226−6232.
(32) Akhter, M. S.; Alawi, S. M. A comparison of micelle formation of ionic surfactants in formamide, in N-methylformamide and in N,N-dimethylformamide. *Colloids Surf., A* **2003**, *219*, 281−290.
(33) Ruiz, C. C.; Díaz-López, L.; Aguiar, J. Self-assembly of tetradecyltrimethylammonium bromide in glycerol aqueous mixtures: A thermodynamic and structural study. *J. Colloid Interface Sci.* **2007**, *305*, 293−300.
(34) Greaves, T. L.; Weerawardena, A.; Drummond, C. J. Nanostructure and amphiphile self-assembly in polar molecular solvents: amides and the "solvophobic effect". *Phys. Chem. Chem. Phys.* **2011**, *13*, 9180−9186.
(35) Wijaya, E. C.; Greaves, T. L.; Drummond, C. J. Linking molecular/ion structure, solvent mesostructure, the solvophobic effect and the ability of amphiphiles to self-assemble in non-aqueous liquids. *Faraday Discuss.* **2013**, *167*, 191−215.
(36) Ray, A. Solvophobic interactions and micelle formation in structure forming nonaqueous solvents. *Nature* **1971**, *231*, 313−315.
(37) Ronis, D.; Martina, E.; Deutch, J. M. The solvophobic effect in simple fluid mixtures. *Chem. Phys. Lett.* **1977**, *46*, 53−55.
(38) Stuart, M. C. A.; Van de Pas, J. C.; Engberts, J. B. F. N. Phase behavior of laundry surfactants in polar solvents. *J. Surfactants Deterg.* **2006**, *9*, 153−160.
(39) Moyá, M. L.; Rodríguez, A.; del Mar Graciani, M.; Fernández, G. Role of the solvophobic effect on micellization. *J. Colloid Interface Sci.* **2007**, *316*, 787−795.
(40) Macosko, C. W. *Rheology: Principles, Measurements, and Applications*; Wiley-VCH: New York, 1994.
(41) Larson, R. G. *The Structure and Rheology of Complex Fluids*; Oxford University Press: New York, 1999.
(42) Koehler, R. D.; Raghavan, S. R.; Kaler, E. W. Microstructure and dynamics of wormlike micellar solutions formed by mixing cationic and anionic surfactants. *J. Phys. Chem. B* **2000**, *104*, 11035−11044.
(43) Bijma, K.; Engberts, J. B. F. N. Effect of counterions on properties of micelles formed by alkylpyridinium surfactants .1. Conductometry and H-1-NMR chemical shifts. *Langmuir* **1997**, *13*, 4843−4849.
(44) Lane, L. B. Freezing points of glycerol and its aqueous solutions. *Ind. Eng. Chem.* **1925**, *17*, 924.
(45) Pedersen, J. S.; Schurtenberger, P. Scattering functions of semiflexible polymers with and without excluded volume effects. *Macromolecules* **1996**, *29*, 7602−7612.
(46) Pedersen, J. S. Analysis of small-angle scattering data from colloids and polymer solutions: modeling and least-squares fitting. *Adv. Colloid Interface Sci.* **1997**, *70*, 171−210.
(47) Glatter, O. New method for evaluation of small-angle scattering data. *J. Appl. Crystallogr.* **1977**, *10*, 415−421.
(48) Ogunsola, O. A.; Kraeling, M. E.; Zhong, S.; Pochan, D. J.; Bronaugh, R. L.; Raghavan, S. R. Structural analysis of "flexible" liposome formulations: new insights into the skin-penetrating ability of soft nanostructures. *Soft Matter* **2012**, *8*, 10226−10232.

DOI: 10.1021/acs.langmuir.9b02125
Langmuir 2019, 35, 12782−12791

Supporting Information for:

Wormlike Micelles of a Cationic Surfactant in Polar Organic Solvents: Extending Surfactant Self-Assembly to New Systems and Sub-Zero Temperatures

Niti R. Agrawal[1], Xiu Yue[1,2], Yujun Feng[3]* and Srinivasa R. Raghavan[1]*

[1]Department of Chemical & Biomolecular Engineering, University of Maryland, College Park, Maryland 20742, USA

[2]Xinjiang Technical Institute of Physics & Chemistry, Chinese Academy of Sciences, Urumqi 830011, China

[3]Polymer Research Institute, State Key Lab of Polymer Materials Engineering, Sichuan University, Chengdu 610065, China

*Corresponding authors. Email: sraghava@umd.edu, yjfeng@scu.edu.cn

Figure S1. Vial photos showing coacervation of EHAC/NaTos samples in glycerol. Samples of EHAC/NaTos in glycerol show a 2-phase region, as discussed in Figure 3 of the main paper. Photos of selected samples are shown here. The samples contain 60 mM EHAC and varying NaTos (120, 150, 180, 240 and 300 mM). All samples show two co-existing liquid phases, i.e., coacervation. The phase boundary between the surfactant-rich phase (bluish) and the salt-rich phase (colorless) is indicated in each sample by a line for clarity.

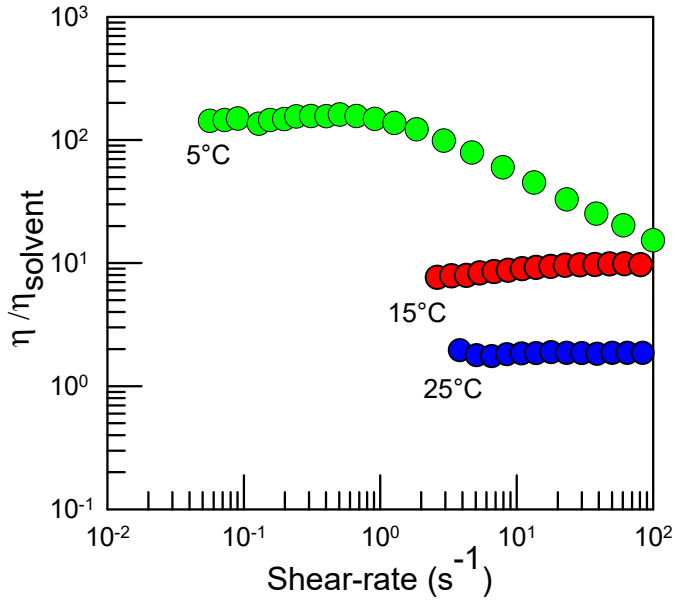

Figure S2. Viscosity data in formamide at different temperatures. The relative viscosity data for a sample of 60mM EHAC + 90 mM NaSal in formamide is shown at different temperatures of 25, 15 and 5°C. The data at 5°C alone is plotted in Figure 6 of the main paper. Note that the sample remains Newtonian at 15 and 25°C while it is shear-thinning at 5°C.

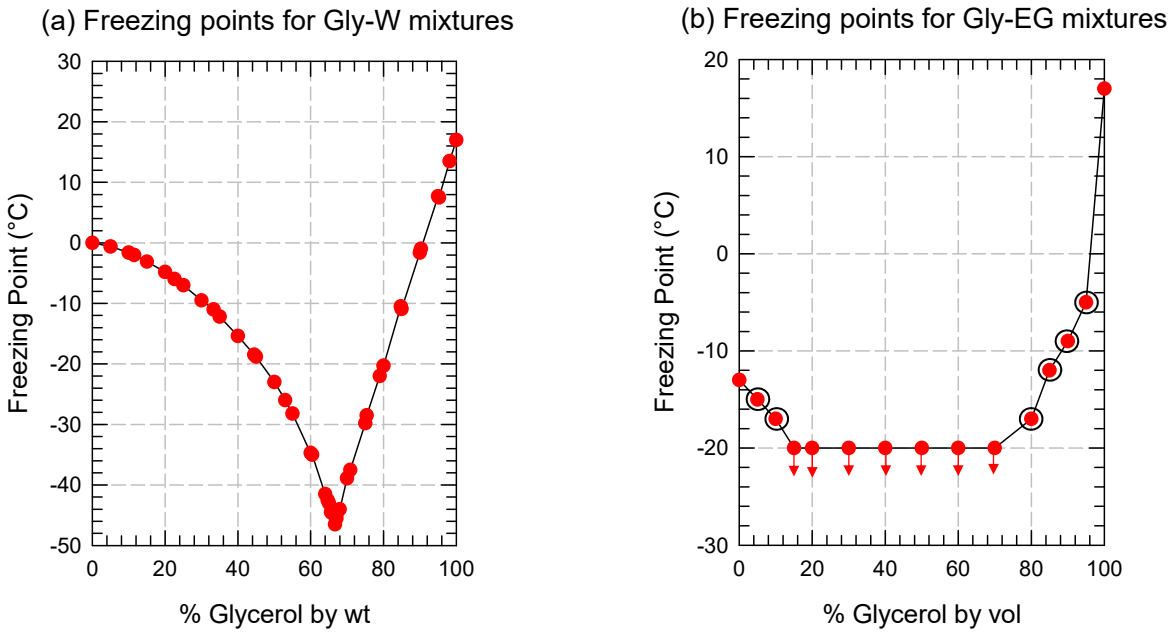

Figure S3. Freezing points of mixtures containing glycerol (Gly). The freezing points of glycerol-water (Gly-W) mixtures (a) and glycerol-ethylene glycol (Gly-EG) mixtures (b) are shown here. Gly-water data are replotted from Ref. 38. For Gly-EG mixtures, the samples were observed at –20°C (freezer) and –5°C (circulating bath), and the phase (solid or liquid) was estimated from the flowability of the sample. The red arrows indicate a freezing point below –20°C, i.e., the sample remained liquid under these conditions. The points with black circles are interpolated values for the freezing points between –5 and –20°C.

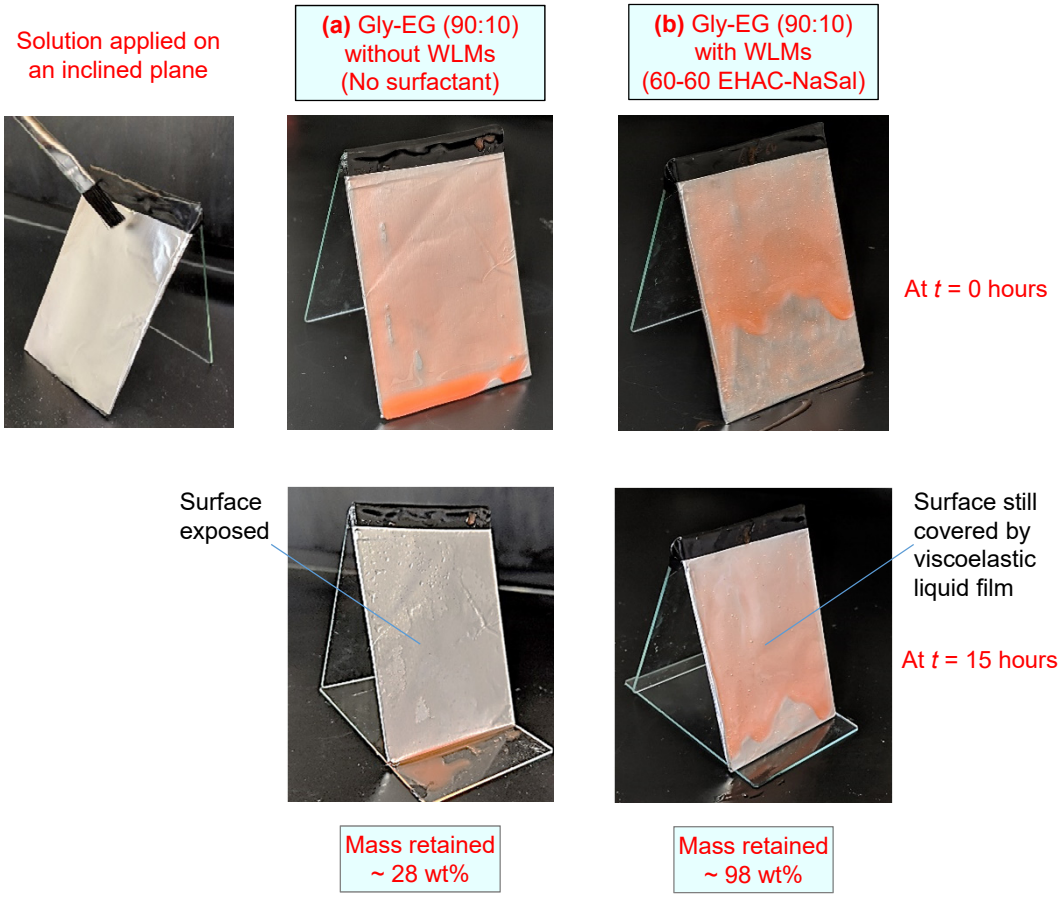

Figure S4. Experiment demonstrating the utility of viscoelastic WLMs in Gly-EG mixtures. A Gly-EG (90:10 v/v) mixture has a freezing point below –20°C. It can be rendered viscoelastic (due to the formation of WLMs) by adding EHAC-NaSal (60-60 mM). The bare solvent mixture and its viscoelastic counterpart are compared in a simple visual test. For this, inclined aluminum surfaces were created using glass slides covered with aluminum foil. Red iron oxide pigment (0.1 wt%) was added to the solutions for better visualization. Approximately 1 g of the respective samples were applied onto the surfaces using a paint brush (left top) at time t = 0, and the surfaces were then placed in the freezer (T ~ –20°C) for 15 hours. Due to the low freezing point of the solvent, neither sample froze into a solid. Results are shown in (a) for the Gly-EG solvent mixture and in (b) for the viscoelastic sample of WLMs in Gly-EG. In (a), the liquid initially coats the surface (top), but it quickly flows down the surface and collects in a pool below (bottom). The surface is thereby left exposed. Only 28% of the liquid mass was measured to remain on the surface. In (b), the viscoelastic sample coats the surface as a thin film (top), and this film persists even after 15 hours (bottom). 98% of the sample mass was found to remain on the surface.

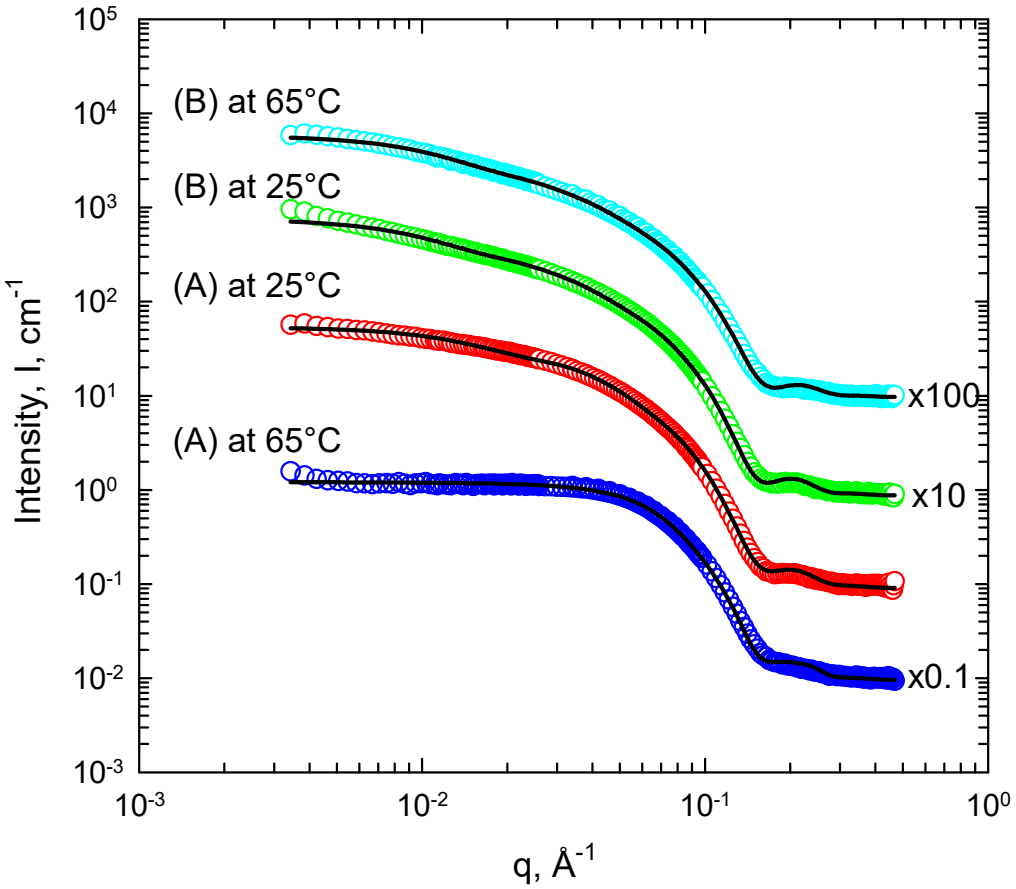

Figure S5. Model fits to SANS data shown in the paper. Plots of scattered intensity I vs. wave-vector q are shown for sample A (EHAC-NaSal 60-30 mM) and sample B (EHAC-NaSal 60-60 mM) at two different temperatures: 25 and 65°C. In each case, the data (open circles) are fit to a model, and the model fits are shown as continuous lines. The model is discussed below on page S-7. Parameters corresponding to the fits are shown in the table below.

Table S1. Fitting parameters for the data in Figure S5.
The selected model is for cylinders having a polydisperse radius and interacting via hard-sphere interactions.

Sample EHAC-NaSal (mM)	Temp (°C)	Radius (Å)	Distribution of Radius	Length (Å)	Volume Fraction	Reduced χ^2
60-30	25	23.9	0.105	336	0.057	35.8
	65	23.5	0.088	93	0.076	33.5
60-60	25	24.0	0.096	473	0.036	33.2
	65	22.7	0.102	425	0.028	27.1

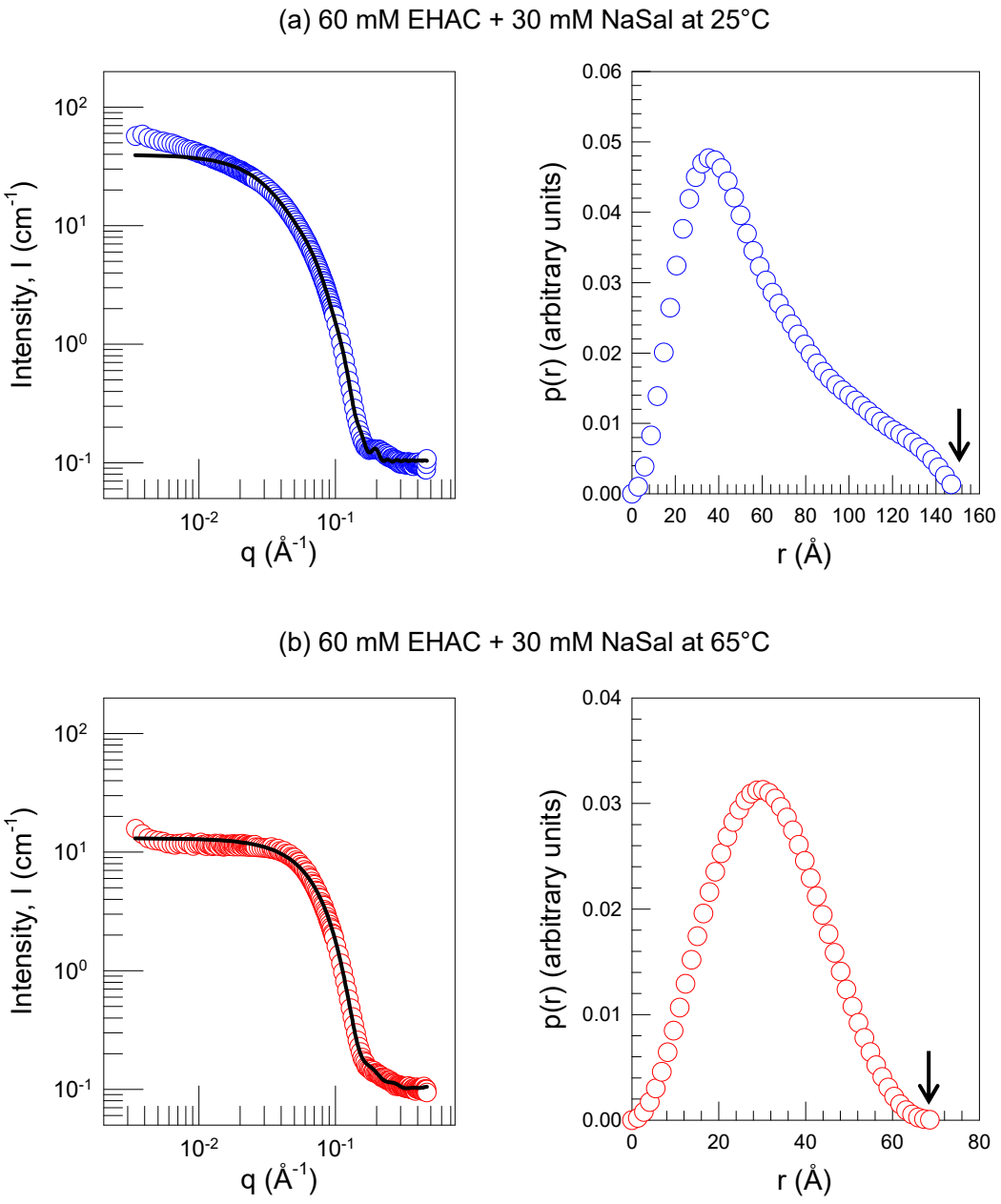

Figure S6. IFT analysis of SANS data shown in the paper. The SANS data for the sample of EHAC-NaSal (60-30 mM) in glycerol at 25°C and 65°C are analyzed by the IFT method (see page S-7 below) to obtain the corresponding pair distance distribution functions *p*(*r*). (a) At 25°C, the *p*(*r*) plot is asymmetrical and indicative of elongated micelles (WLMs). The point where *p*(*r*) hits the x-axis (~ 150 Å), indicated by the arrow, is an estimate for the micellar length. (b) At 65°C, on the other hand, *p*(*r*) is symmetrical, which is indicative of spherical micelles. The point where *p*(*r*) hits the x-axis (~ 70 Å), indicated by the arrow, is an estimate for the micellar diameter.

SANS Modeling (Figure S5): SANS data in the figure were fit using a model available in the SasView software package provided by NIST. This model is described by equations S1 to S6. It models the structures in the sample as cylinders interacting via hard-sphere interactions. The cylinders are modeled as being polydisperse in their radius, but monodisperse in their length. Fitting parameters from the model fits are provided in Table S1.

The form factor $P(q)$ in the model accounts for the size and shape of the scatterers. For cylinders of radius r and length L, it is given by the following (see Refs. 45, 46 in the main paper):

$$P(q) = \frac{\text{scale}}{V_{cyl}} \int_0^{\pi/2} F^2(q,\alpha) \sin\alpha \, d\alpha \tag{S1}$$

where the scattering amplitude F is given by:

$$F(q,\alpha) = 2V_{cyl}\left(\rho_{cyl} - \rho_{solv}\right) j_0\left(\frac{qL}{2}\cos\alpha\right)\left[\frac{J_1(qr\sin\alpha)}{qr\sin\alpha}\right] \tag{S2}$$

Here, 'scale' is the volume fraction of cylinders, $V_{cyl} = \pi r^2 L$ is the volume of each cylinder, $j_0(x) = \sin(x)/x$, J_1 is the first-order Bessel function, and α is the angle between the cylinder axis and the scattering vector q. ρ_{cyl} and ρ_{solv} are the scattering length densities of the cylinder and the solvent. To account for polydispersity in the radius, $P(q)$ is averaged over a Schulz distribution of the cylinder radius. The size-averaged $P(q)$ is given by the following, where $f(r)$ is the normalized Schulz distribution of the radius r and V_{poly} is the volume of the polydisperse object.

$$\bar{P}(q) = \frac{1}{V_{poly}} \int_0^x P(q) f(r) dr \tag{S3}$$

Next, the structure factor $S(q)$ accounts for interactions between the cylinders:

$$S(q) = 1 + 4\pi n_p \int_0^{\infty} [g(r) - 1] \frac{\sin qr}{qr} r^2 dr \tag{S4}$$

Here $g(r)$ represents the pair correlation function and n_p is the number of particles (scatterers) per unit volume. Various models for $S(q)$ are available in SasView. We have used the simplest one, which assumes that the particles are 'hard spheres', i.e., that they have no interaction at long distances and an infinite repulsion upon contact (see Ref. 45).

SANS Analysis by IFT (Figure S6): SANS data in the figure were analysed by the IFT approach through the SasView software package provided by NIST. In IFT, a Fourier transformation of the scattering intensity $I(q)$ is performed to obtain the pair distance distribution function $p(r)$ in real space (with r being distance in real space). $p(r)$ provides structural information about the scatterers, such as their shape and maximum dimension. The relationship between $I(q)$ and $p(r)$ is given by the following equation (see Ref. 47):

$$I(q) = 4\pi \int_0^{\infty} p(r) \frac{\sin(qr)}{qr} dr \tag{S5}$$

The characteristic forms of $p(r)$ for structures such as spherical and cylindrical micelles has been discussed in previous papers (see Ref. 48, for example).